Clays and Clay Minerals, 1970, Vol. 18, pp. 37–46. Pergamon Press. Printed in Great Britain

ADSORPTION STUDIES ON KAOLINITES

MARY K. LLOYD and ROBERT F. CONLEY

Georgia Kaolin Research Laboratories, Elizabeth, N. J. 07207

(*Received* 10 *July* 1969)

Abstract—Adsorption studies have been performed on Georgia kaolins having a broad range of crystallinity and particle size distributions (from 0·1μ to 44μ) using N_2 (78°K.), H_2O (273°K.), and $BuNH_2$ (298°K.). Using both vapor and liquid phase adsorption techniques, surface affinities of the adsorbates were determined.

Modified Frenkel–Halsey–Hill plots were used to compute the preferential adsorptivity of H_2O vapor over N_2 (hydrophilicity index, H.I.) as a function of crystallinity index, C.I., and particle size. For amine adsorptivity, non-aqueous adsorption isotherms were obtained.

Within any geographic deposit, crystallinity exhibits an inconsistent pattern with respect to particle size. A single generality is the tendency for crystallinity to increase toward the fine particle size range, $D \rightarrow 0{\cdot}2\mu$. Adsorptivities of N_2, H_2O, and $BuNH_2$ show no dependence upon crystallinity within a given particle size range. However, F.H.H. compensated slopes, describing the preferential adsorptivity over N_2, show a definite decrease as crystallinity increases. A striking anomaly occurs in the vicinity of $0{\cdot}2 <$ C.I. $< 0{\cdot}7$ where H.I. increases briefly then returns to the original trend. The rate of decrease of H.I. vs. C.I. is consistently steeper with increasing particle size. Adsorption of water vapor most likely occurs as a 1 : 1 configuration on each silica-alumina edge group, 1 : 1 on each basal silica, and 1 : 2 (hindered configuration) on each basal alumina group.

The data suggest that amines adsorb preferentially and quantitatively on the edges, i.e. the Lewis and Bronsted acid sites, and follow a Langmuir pattern.

1. INTRODUCTION

THE BEHAVIOR of clay minerals, both chemically and physically, depends to a great extent upon their surface energetics, due in part to surface area and degree of mineral perfection. In kaolins, for example, pigmentary and rheological properties are influenced mainly by these parameters.

To define more clearly the role of surface character on adsorption, from which many kaolin properties derive, adsorption studies were performed on very diverse types of Georgia kaolins. A prime difficulty in interpreting data on kaolins, particularly those reported for single or small-suite samples, lies in associating the phenomena with their causes. Georgia kaolins, while reasonably pure, vary considerably in particle size, particle shape (Conley, 1966), crystallinity (Hinckley, 1965), and impurity content, both adsorbed, e.g. organic lignins and tannin, and extraneous, as micas, montmorillonites, quartz, etc. (Bates, 1967). Thus, adsorptivity measurements will reflect various phenomenologies. Though some work has been reported on contaminant removal (Langston, *et al.*, 1966), it has not been practicable to obtain an impurity-free, physically unaltered kaolin specimen.

The present work represents an attempt to ascertain more accurately the functionality of the kaolin surface, *per se*, in adsorptivity. By use of broadly variant kaolins and regression analysis with central limit bias (Univac 1108 programs), adsorptivity with varying adsorbate polarities was studied.

2. EXPERIMENTAL

Gas adsorption isotherms employing nitrogen at −196°C, water vapor at 0°C, and solution adsorption isotherms with butylamine in water-free heptane at 25°C were obtained, using conventional B.E.T. and Langmuir techniques and a Micromeretics 103 surface area analyzer. Thermodynamic evidence shows nitrogen, a non-polar molecule, to adsorb on both hydrophilic and hydrophobic areas. Water adsorption information was collected because many kaolin applications lie in aqueous systems. Polyamines are employed commercially to disperse kaolin in aqueous systems where subsequent interaction with various organic compounds (Bundy, 1963, Dohman, 1967) is required. Also, aliphatic amines are employed for introducing hydrophobic character to clay surfaces (Jordan, 1949). For these reasons, amine adsorption carries considerable interest. Butylamine was chosen as an adsorbate because of its appreciable solubility in both heptane and water, an analytical necessity. An anhydrous solvent was chosen to avoid competitive adsorption effects contributed by an aqueous environment.

The kaolins selected were representative mine

https://doi.org/10.1346/CCMN.1970.0180105 Published online by Cambridge University Press

samples from the Georgia area having a broad and continuous range of crystallinities and particle sizes. The crystallinity index, as defined by Johns and Murray (1956), varied from 0·0 → 1·0, and the particle size from 0·1μ → 44μ. The samples were centrifugally classified on production equipment into four general particle size ranges (see Table 1) representative of commercial processing. While very narrow size fractions might prove advantageous in adsorption studies, they are exceedingly difficult to prepare in quantities greater than milligrams. Further, it was expected that results from this work could be directly applied to materials of commerce and problems of industry.

Table 1. Particle size classification of kaolins

Kaolin	Median particle size (μ)	% < (1μ)*
A	7·0–9·0	7
B	0·7–0·9	61
C	0·3–0·5	86
D	0·2–0·3	94

*All samples were 100 per cent < 44μ.

The kaolins were converted to the hydrogen form by elutriation with H_2SO_4 at pH 3, water washed, dried at 125°C, cooled under desiccation, and adsorption studies performed immediately thereafter. Hydrogen clays were chosen to obtain unequivocal results with amine adsorption and to clarify the location of acid sites on kaolinite. While hydrogen clays are believed to transform to the aluminum form in time, aging studies showed no variation in N_2, H_2O or $BuNH_2$ adsorption beyond that ascribable to analytical error (<1 per cent).

Crystallinity index, C.I., as employed in this work, is an empirical measurement proposed by Johns and Murray (1959) and is the ratio of the intensities of $02\bar{1}$ and 060 kaolinite reflections in a randomly oriented sample. This intensity ratio is believed to measure primarily the randomness in "*b*" axis shift. The kaolins chosen for this work were selected for a continuous crystallinity range. Thus, the discontinuity in crystallinity index around 0·5–0·8, as reported by Johns and Murray with their random clay sampling, did not appear.

As crystallinity may vary geographically and stratigraphically, distributions of crystallinities can exist in any broad mine sampling, e.g. the materials in this study. Random mixtures of good and poor crystalline kaolins should produce a continuous series of crystallinity indices. Thus, no certainty of association exists between lateral or vertical displacements or particle size distributions. Hence, a given index likely measures mixtures of crystals within a sample possessing various degrees of "*b*" shift.

3. RESULTS

Within any single mine sampling, as shown in Table 2, crystallinity varies inconsistently with particle size. However, over all samples, crystallinity increases qualitatively with decreasing particle size (Ormsby and Marcus, 1964) as reflected by the *t* test for validity. Crystallinity and particle size are well known influential factors in adsorption (poor crystallinity tends to restrict particle growth which is, in turn, associated with higher surface area).

Table 2. Crystallinity index variation in mine deposits and particle size

Mine* location	Particle size fraction (from Table 1) *A* > *B* > *C* > *D*
I	0·15 0·61 0·16 0·27
II	0·17 0·67 0·49 0·59
III	0·20 0·14 0·10 0·18
IV	0·20 0·36 0·45 0·33
V	0·25 0·27 0·29 0·41
VI	0·46 0·48 0·73 0·55
VII	0·61 0·87 0·43 1·00

*All mine areas in central Georgia, (fall line).
C.I. for all members = 0·41. *t*, test for crystallinity/particle size correlation, (96 per cent confidence level) = 2·75.

Water adsorption

Modified Frenkel–Halsey–Hill plots, a means of determining surface affinity for gaseous adsorbates, were used to study the relative adsorptivity of

https://doi.org/10.1346/CCMN.1970.0180105 Published online by Cambridge University Press

water vapor and nitrogen, based on the success of Zettlemoyer (1968), Pierce (1968), and others in predicing surface character. In this technique, a slope is obtained from a data plot of volume adsorbed (or millimoles) vs. log partial pressure of adsorbate. By selecting the proper partial pressure region from initial B.E.T. plots, monolayer or multilayer adsorption can be studied.

The ratio of slopes for water to nitrogen was computed, each determined with a minimum of five data points and overall confidence level of 99·9 per cent. This ratio measures the relative affinity of the surface for water over nitrogen at their respective temperatures, and is termed the *Hydrophilicity Index*, H.I.

$$\text{H.I.} = \frac{\Delta \text{ moles } H_2O \text{ ads.}}{\Delta \log P/P_{s(H_2O)}} \Big/ \frac{\Delta \text{ moles } N_2 \text{ ads.}}{\Delta \log P/P_{s(N_2)}}.$$

The data for the 28 samples showed random scatter and gave no evidence of positive correlation between H.I. and organic content, either with carbon alone (graphitic impurity) or with carbon and hydrogen (carbonaceous impurity). A computed average area covered by the organic constituent, assuming a monolayer distribution, is approximately 1–2 M^2/g, a small but significant fraction of the total surface area exhibited by water (3–16 M^2/g). Yet, these data do not support the suggestion that the presence of naturally occurring organic impurities on a kaolin surface reduces detectably that surface's affinity for water as compared to nitrogen. Non-interference may be variously interpreted. Organic materials may adsorb at locations distinctly separate from H_2O, whether on kaolin or on the accessory minerals. Adsorption of carbonaceous matter on interlaminar surfaces could block easily further adsorption of both H_2O and N_2. A second explanation lies in a more globular structure for the organic impurity, of a size which would contribute or block very little surface area. Based on the chemical analyses, a mean globular size of only 50 Å for the organic matter would reduce its effective surface to less than one-tenth of the monolayer value. It is not likely that either this size or area would be perceptible by electron micrographic or surface area examination.

For purposes of interpretation of water adsorption on kaolin surfaces, the fraction of the surface on which organic contaminant interferes may, therefore, be neglected.

In the plot of crystallinity index vs. organic content, Fig. 1, high crystallinity index materials show somewhat less contamination by statistical analysis than low index ones. Such a relation might be anticipated on the basis of higher surface energy on low crystallinity materials. However, the relationship is not pronounced.

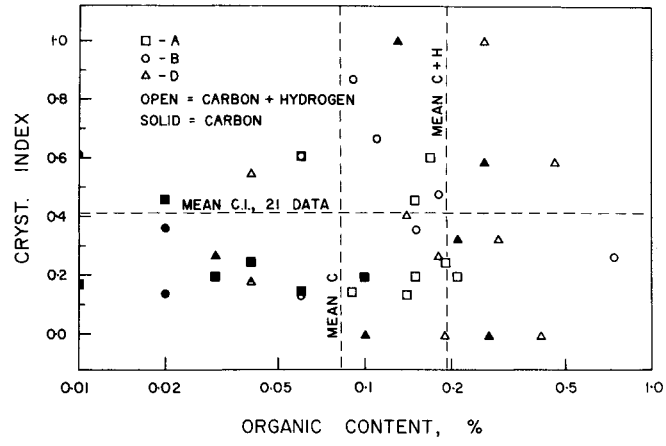


Fig. 1. Association of organic contamination with crystallinity (Index, I_{021}/I_{060}).

In Figs. 2 and 3, a trend exists towards higher hydrophilicity with poorer crystallinity for all particle size fractions, in both monolayer ($P/P_{sat.} \simeq 0{\cdot}10$) and multilayer ($P/P_{sat.} \simeq 0{\cdot}35$ adsorption. In poorer crystallinity clays, the *b*-axis displacement of layers (Brindley, 1951; Brindley and Nakahira, 1958) could generate edge displacements, and, hence, contribute high energy sites.

The slope of hydrophilicity index vs. crystallinity index is steepest with the coarsest fraction, *A*, and decreases progressively with finer particle size. This would be explained, in part, by the *A* fraction, which contains more blocky particles, having the

https://doi.org/10.1346/CCMN.1970.0180105 Published online by Cambridge University Press

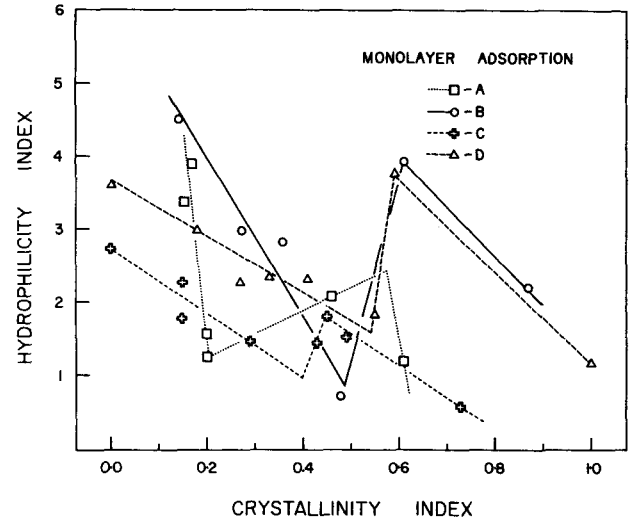


Fig. 2. Variation of monolayer hydrophilicity with crystallinity (Index, I_{021}/I_{060}) and particle size.

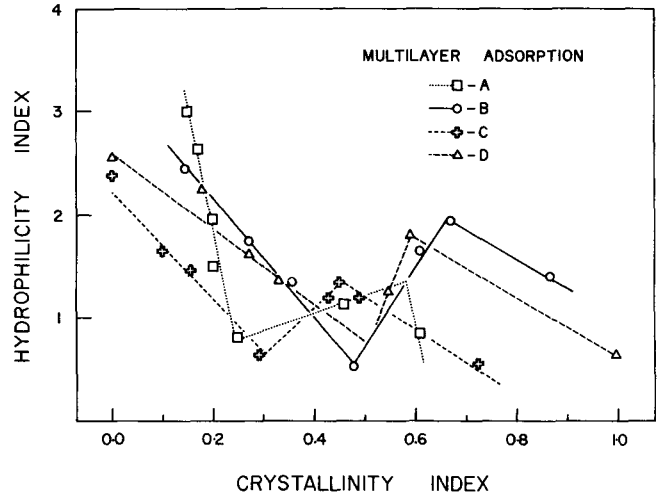


Fig. 3. Variation of multilayer hydrophilicity with crystallinity (Index, I_{021}/I_{060}) and particle size.

greatest ratio of edge to total surface. A discontinuity in the slopes occurs between 0·3 and 0·6 crystallinity index with all particle size fractions, both in monolayer and multilayer adsorption. Following this break, the slope again reverses to about its original value, considering the sparcity of data near the high C.I. region. The discontinuity appears to be related to crystallinity and not to particle size. For example, *C* samples generally have lower crystallinity indices than *B* and *D* and higher values than *A*. However, the knee of the early break in *C* precedes both *B* and *D* but follows *A*.

Hydrophilicity index values for monolayer coverage are consistently higher than for multilayer, which suggests the operation of dipole-dipole forces at the high energy sites, whose magnitude decreases rapidly with distance*. Thus, the affinity for adsorbate at approximately 3 layers ($P/P_{sat.} \simeq 0{\cdot}3$), while decreased, is still significant. At much higher adsorption pressures, where 5–10 layers form, the attractive influence of the surface (and

*Dipole-dipole interactions vary inversely as the seventh power of the distance.

https://doi.org/10.1346/CCMN.1970.0180105 Published online by Cambridge University Press

the anomaly in the H.I. vs. C.I. slopes) is obscured.

The adsorption of water on the various surfaces of clay minerals has been the subject of much investigation (Johansen and Dunning, 1959; Keenan, Moody, and Wood, 1951; Martin, 1959; Orchistron, 1954; Sposito and Babcock, 1966; Van Olphen, 1965). The adsorption isotherm is not sufficiently definitive, even by the sophisticated methods of Ross (1964), to properly locate water molecules during monolayer coverage. However, a comparison of water vs. nitrogen adsorbed at monolayer coverage for a wide variety of kaolins should yield some insight into this problem.

Independently of the location and mechanism of molecular adsorption, the molar adsorption index for water vs. nitrogen, $M.A.I._{H_2O/N_2}$, is given by

$$M.A.I._{H_2O/N_2} = \frac{\Sigma f_{H_2O} C_{H_2O}}{f_{\Sigma N_2} C_{N_2}}$$

where f = effective area exhibited by a given molecule on a given surface in Å/molecule
C = number of molecules on that surface.

The effective area for nitrogen is an empirically determined number, varying slightly with the substrate (Livingston, 1959). For kaolins a value of 15·8 Å^2 for N_2 represents an overall average for the various surfaces. The surface area of kaolinite particles may be computed accurately from electron micrographic surveys.

(1) The basal area for an isogonic, anisometric hexagon, is given by

$$A_b = \frac{\sqrt{3}}{2} a \times b^*$$

where a and b are the major and minor dimensions normal to an edge.

(2) The prism faces (edge surface) contribute an area

$$A_e = \sqrt{3} c(a+b)^*$$

where c is a thickness dimension normal to a and b.

(3) Another defining characteristic of particle geometry which may affect adsorption is the shape factor, ϕ, given by

$$\phi = \frac{c}{\sqrt{a \times b}}$$

and is determined from shadowed electron micrograph measurements.

Table 3 contains various adsorption models, effective areas, shape factors, and predicted values for $M.A.I._{H_2O/N_2}$ based thereon. The value of $\phi = 0{\cdot}16$ is an average for various C and D fractions (Conley, 1966) while 0·30 is representative, though less consistently, of the A fraction ($> 5\mu$).

While other adsorption models are theoretically possible, they either are mathematically more remote or no thermodynamic evidence has been given in their support. Model 4 is the conclusion by Sposito and Babcock (1966) following treatment of the energetics of adsorption by a modification of the Schroedinger quantum energy equation. Terms are included for the various vibrational modes of the H_2O molecules and van der Waals molecule–crystal surface interactions. Solved for the potential energy minima, the set of equations predicts the most probable molecule orientation of water on the various kaolinite faces. Model 1 is derived by Hendricks and Jefferson (1938) from ice configurations.

The fourteen C and D particle size samples are represented in the mole adsorbent plot, Fig. 4. The slope for these data represents an experimental determination of $M.A.I._{H_2O/N_2}$. The best fit of a line through the origin yields a slope of 0·64, a value quite close to the adsorption mechanism in Model 4. Thus, the present experimental data strongly support the theoretical work of Sposito and Babcock.

Butylamine adsorption

Adsorptivity of butylamine on the kaolin surface, like adsorptivity of water, shows no positive correlation with the organic contaminant, even at increased levels of organic content. Further, no relation is extant between the adsorptivity for butylamine, K_{BuNH_2}, on kaolin surfaces and crystallinity index. This may be due in part to the use of a non-aqueous medium for $BuNH_2$, as opposed to pure gas adsorption for N_2 and H_2O. While it is not rational to relate the Langmuir adsorptivity factor, K, to the N_2 and H_2O volume/partial pressure slopes on a quantitative basis, some general observations can be made.

The quotient, K/moles N_2 ads./log $P_0/P_{sat.\,N_2}$ is a qualitative measure of the affinity, per unit surface, of the various clays for butylamine and circumvents inherent surface area effects. Table 4 contains the crude data distribution for all members of Table 2 in three subranges of crystallinity.

Though no firm conclusions can be drawn, some indication exists that surface affinity for butylamine is high with both poor and well crystalline kaolins

*These formulas hold accurately for hexagons where the digression from regularity is $a/b < 2$.

https://doi.org/10.1346/CCMN.1970.0180105 Published online by Cambridge University Press

Table 3. Molar adsorption indices for various H_2O adsorption models

Model	Mole ratio of adsorbate/surface atom for H_2O adsorption	f_{H_2O},* Å²/molecule	ϕ	Predicted M.A.I.$_{H_2O/N_2}$
1	1–1, SiO basal	11·2	0·16	0·939
	1–1, AlOH basal	11·2	0·30	0·908
	1–1, SiO–AlOH edge	16·0		
2	1–1, SiO basal	11·2	0·16	0·844
	1–1, AlOH basal	11·2	0·30	0·766
	1–1, SiO or AlOH edge	32·0		
3	1–1, SiO basal	11·2	0·16	0·752
	1–2, AlOH basal	22·4	0·30	0·752
	1–1, SiO–AlOH edge	16·0		
4	1–1, SiO basal	11·2	0·16	0·657
	1–2, AlOH basal	22·4	0·30	0·610
	1–1, SiO or AlOH edge	32·0		
5	1–1, SiO basal	11·2	0·16	0·750
	1–1, AlOH basal	11·2	0·30	0·625
6	1–1, SiO or AlOH edge	32·0	0·16	0·094
			0·30	0·142

*Brindley and Robinson (1946), Newnham and Brindley (1956).

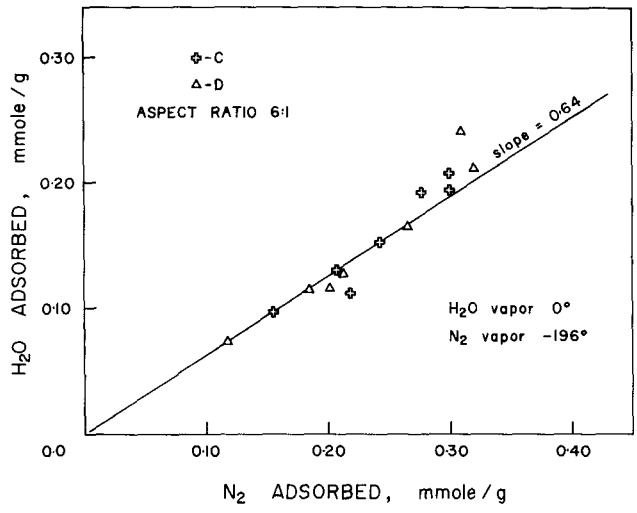


Fig. 4. Linear relationship between nitrogen and water vapor adsorption for monolayer coverage.

and low in the mid range. This trait is not dissimilar to the surface affinity for water.

Adsorption mechanisms for $BuNH_2$ and H_2O appear quite different. Theoretical slopes for various models of surface coverage by $BuNH_2$, assuming 25 Å² for the area of butylamine molecule (Betts and Pethica, 1956) and 15·8 Å² for nitrogen, are itemized in Table 5.

https://doi.org/10.1346/CCMN.1970.0180105 Published online by Cambridge University Press

Table 4. Relative surface affinity of butylamine on various clays

Crystallinity range	Statistical weighting	Per cent distributed above median $BuNH_2$ affinity	Per cent distributed below median $BuNH_2$ affinity
0·00–0·33	43%	67	17*
0·33–0·67	43%	33	67
0·67–1·00	14%	100	0

*Two data points in this range fell on the median.

Table 5. Molar adsorption indices for various $BuNH_2$ adsorption models

Model	Mole ratio of adsorbate surface atom for $BuNH_2$ adsorption	f_{BuNH_2} Å²/molecule	ϕ	Predicted M.A.I.$_{BuNH_2/N_2}$
7	1–2, SiO basal	22·4	0·16	0·571
	1–2, AlOH basal	22·4	0·30	0·605
	1–1, SiO or AlOH edge	32·0		
8	1–2, SiO basal	22·4	0·16	0·375
	1–2, AlOH basal	22·4	0·30	0·312
9	1–1, SiO or AlOH edge	32·0	0·16	0·195
			0·30	0·293

In Fig. 5, butylamine vs. nitrogen for monolayer coverage, the best straight lines through the origin for the experimental data for *A* and *B* fractions and *C* and *D* fractions have slopes of 0·30 and 0·20, respectively. Characteristically, butylamine is known to adsorb on Lewis or Bronsted acid sites, as demonstrated by Benesi (1957) using Hammett indicators, and acid sites on kaolin are primarily on edge faces (Hertl and Hair, 1968, Peri, 1966, Solomon and Rosser, 1965). With 6:1 platelet geometry for *C* and *D* fractions and the assumption that butylamine adsorbs only one molecule per Al–Si edge group, the computed slope for Model 9, 0·195, lies very close to the observed 0·20. The experimental slope value 0·30 for the *A* and *B* fractions, by the same reasoning, is represented well by the predicted value, 0·293, for $> 5\mu$ fractions. Thus, it seems evident that butylamine adsorbs primarily, if not exclusively, on the edge faces.

If butylamine adsorbs essentially on the edge faces of kaolin and if a differential affinity for $BuNH_2$ exists throughout the crystallinity range, as shown qualitatively previously, it is probable that surface acid strength is influenced by crystallinity. Further support is lent by titration studies (Conley and Golding, 1959) of kaolins with bases of varying dissociation constants. The slope of pH vs. base added, both early in the titration and near the equivalence point, is a measure of the K_a of the kaolin acid groups. These data strongly suggest that clays with low and high C.I. values are associated with higher K_a values (stronger acid groups) than mid range C.I. ones.

Present evidence is too meager to define precisely the mechanism for acidity variance. Likely, it lies in alteration, incomplete and hindered coordination and crystal field effects on surface structures generated by crystallinity and *b* axis dislocations. Continued work is in progress in this area.

4. SUMMARY

The behavior of the kaolin surface with respect to the adsorption of nitrogen, water and butylamine is diverse. Thermodynamic evidence points to a uniform molecular distribution for the non-polar N_2 molecules partly as the result of extremely low temperature adsorption. The highly polar, but neutral, water molecules have a restricted configuration at 0°C. Their adsorption behavior fits the theoretical proposals of Sposito, i.e. 1 molecule per basal silicon atom, 1 molecule per two basal

https://doi.org/10.1346/CCMN.1970.0180105 Published online by Cambridge University Press

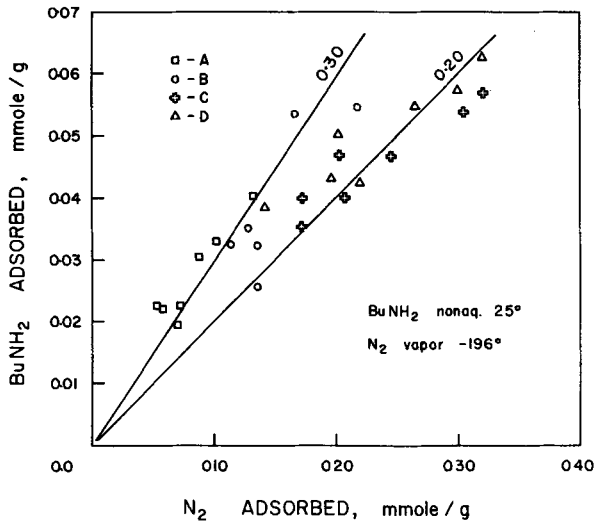


Fig. 5. Linear relationships between butylamine and nitrogen adsorption for monolayer coverage.

aluminum atoms, and 1 molecule per edge aluminum –silicon group. Butylamine, a stronger electron pair donor, chemisorbs at the acidic sites, essentially the incompletely coordinated, edge aluminum atoms. In very poorly crystalline kaolins, slightly more butylamine adsorbs than predicted, which suggests the presence of basal acidic sites.

Both water and butylamine show an adsorption anomaly in the mid range of crystallinity as measured by the criterion of Johns and Murray. The consistency of the pattern points to a structural factor influential in the coordination of polar molecules on kaolin surfaces.

Organic material, e.g., graphite, tannins, and lignins are present in nearly all kaolin deposits. However, even in concentrations up to 1 per cent, their effective surface produces little or no interference in the adsorption of polar molecules.

Acknowledgment—The authors gratefully acknowledge the analytical services of Dr. W. D. Johns in performing crystallinity measurements, and of Maynard Coller and Roy Booth for chemical analyses pertinent to this study.

REFERENCES

Bates, T. F. (1967) Geology and Mineralogy of the Sedimentary Kaolins of the Southeastern United States – a Review: *Clays and Clay Minerals*, 12th Conf. Pergamon Press, New York, 177.

Benesi, H. A. (1957) Acidity of Catalyst Surfaces. II. Amine Titration Using Hammett Indicators: *J. Phys. Chem.* **61**, 970.

Betts, J. J. and Pethica, B. A. (1956) The Ionization Characteristics of Monolayers of Weak Acids and Bases: *Trans. Faraday Soc.* **52**, 1581.

Brindley, G. W. (1951) X-Ray Identification and Structure of the Clay Minerals: *Min. Soc. Gt. Britain, Monograph*, 32.

Brindley, G. W. and Nakahira, M. (1958) Further Consideration of the Crystal Structure of Kaolinite: *Mineral. Mag.* **31**, 781.

Brindley, G. W. and Robinson, K. (1946) The Structure of Kaolinite: *Mineral. Mag.* **27**, 242.

Bundy, W. M. (1963) *U.S. Pat.* 3,080,256.

Conley, R. F. (1966) Statistical Distribution Patterns of Particle Size and Shape in the Georgia Kaolins: *Clays and Clay Minerals*, 14th Conf. Pergamon Press, New York, 317.

Conley, R. F. and Golding, H. J. (1959) unpublished data, Georgia Kaolin Company.

Dohman, E. J. (1967) *U.S. Pat.* 3,298,849.

Hendricks, S. B. and Jefferson, M. E. (1938) Structure of Kaolin and Talc-Pyrophyllite Hydrates and Their Bearing on Water Sorption of Clays: *Am. Mineralogist.* **23**, 863.

Hertl, W. and Hair, M. L. (1968) Hydrogen Bonding between Adsorbed Gases and Surface Hydroxyl Groups on Silica: *J. Phys. Chem.* **72**, 4676.

Hinckley, D. N. (1965) Mineralogical and Chemical Variations in the Kaolinite Deposits of the Coastal Plain of Georgia and South Carolina: *Am. Mineralogist* **50**, 1865.

Johansen, R. T. and Dunning, H. N. (1959) Water Adsorption on Clays: *Clays and Clay Minerals*, 6th Conf. Pergamon Press, New York, 249.

Johns, W. D. and Murray, H. H. (1959) Empirical Crystallinity Index for Kaolinite: *Prog. Abst. Geol. Soc. Am.* **70**, No. 2, 1624.

Jordan, J. W. (1949) Organophilic Bentonites, I. Swelling in Organic Liquids: *J. Phys. Colloid Chem.* **53**, 294. *see also*: Cohn, M. I. (1954) *U.S. Pat.* 2,697,699; Pechukas, A. (1954) *U.S. Pat.* 2,692,871; Brown, W.

https://doi.org/10.1346/CCMN.1970.0180105 Published online by Cambridge University Press

(1956) *U.S. Pat.* 2,761,840; Detrick, S. (1942) *U.S. Pat.* 2,305,379; Caruso, G. P. (1967) *U.S. Pat.* 3,321,398.

Keenan, A. G., Moody, R. W., and Wood, L. A. (1951) The Relation between Exchangeable Ions and Water Adsorption on Kaolinite: *J. Phys. Chem.* **55**, 1462.

Langston, R. B., Jenne, E. A., and Pask, J. A. (1966) Effect of Impurities on the Rheology of Two Kaolins: *Clays and Clay Minerals*, 13th Conf. Pergamon Press, New York, 381.

Livingston, H. K. (1949) The Cross-Sectional Areas of Molecules Adsorbed on Solid Surfaces: *J. Colloid Sci.* **4**, 450.

Martin, R. T. (1959) Water Vapor Sorption on Kaolinite, Hysteresis: *Clays and Clay Minerals*, 6th Conf. Pergamon Press, New York, 259.

Newnham, R. E. and Brindley, G. W. (1956) Structure of Dickite: *Acta Cryst.* **9**, 759.

Orchistron, H. D. (1954) Adsorption of Water Vapor, II. Clays at 25°C: *Soil Sci.* **78**, 463.

Ormsby, W. C. and Marcus, J. H. (1964) Rheological Properties of Kaolins of Varying Degrees of Crystallinity: *Clays and Clay Minerals*, 12th Conf. Pergamon Press, New York, 207.

Peri, J. B. (1966) Infrared Study of Adsorption of Carbon Dioxide, Hydrogen Chloride and Other Molecules on Acid Sites on Dry Silica-Alumina and γ-alumina: *J. Phys. Chem.* **70**, No. 10, 3168.

Pierce, W. C. (1968) The Hill Equation for Adsorption on Uniform Surfaces: *J. Phys. Chem.* **72**, No. 6, 1955.

Ross, S. and Olivier, J. P. (1964) *On Physical Adsorption*, Interscience, New York, 129.

Solomon, D. H. and Rosser, M. (1965) Reactions Catalized by Minerals, Part I Polymerization of Styrene: *J. Appl. Polymer Sci.* **9**, 1261.

Sposito, G. and Babcock, K. L. (1966) Equilibrium Theory of the Kaolinite–Water System at Low Moisture Contents, with Some Remarks Concerning Adsorption Hysteresis: *Clays and Clay Minerals*, 14th Conf. Pergamon Press, New York, 133.

Van Olphen, H. (1965) Thermodynamics of Interlayer Adsorption of Water in Clays, *J. Colloid Sci.* **20**, 822.

Zettlemoyer, A. C. (1968) A Review of Research on Hydrophobic Surfaces: A.C.S. *Symposium on Hydrophobic Surfaces*.

Résumé – On a effectué des études sur l'adsorption des kaolins de Georgie ayant une gamme étendue de distributions de cristallinité et de grandeur des particules (de 0,1 μ à 44μ) utilisant N_2 (78°K), H_2O (273°K) et $BuNH_2$ (298°K). En employant à la fois les techniques d'adsorption de vapeur et en phase liquide, on a déterminé les affinités de surface des produits d'adsorption. Les graphiques modifiés de Frenkel–Halsey–Hill ont servi à calculer l'adsorptivité préférentielle de la vapeur de H_2O sur N_2 (index hydrophilicite, H.I.) comme une fonction de l'index de cristallinité, C.I. et de la grandeur de la particule. Pour l'adsorptivité des amines, on a obtenus des isothermes d'adsorption non-aqueux. En général la cristallinité présente un modèle incompatible à la taille de la particule. Une généralité simple est la tendance de la cristallinité à augmenter vers la gamme de particules de grandeur $\bar{D} \rightarrow 0{,}2\mu$. Les adsorptivités de N_2, H_2O et $BuNH_2$ ne montrent aucune dépendance sur la cristallinité dans une limite donnée de grandeur de particules. Toutefois, les pentes compensées F.H.H., décrivant l'adsorptivité préf'erentielle sur N_2, indiquent une diminution définie au fur et à mesure que la cristallinité augmente. Une anomalie frappante se produit dans le voisinage de $0{,}2 < C.I. < 0{,}7$ où H.I. augmente brièvement et revient ensuite à la tendance initiale. Le taux de diminution de H.I. en fonction de C.I. est plus fort avec le hausse de la grandeur des particules. L'adsorption de la vapeur d'eau se produit, le plus souvent, comme une configuration 1 : 1 sur chaque groupe limite de silice d'aluminium, 1 : 1 sur chaque silice basal et 1 : 2 (configuration entravée) sur chaque groupe d'alumine basale. Les données suggèrent que les amines adsorbent de préférence et quantitativement sur les bords, à savoir les zones acides de Lewis et de Bronsted, et suivent un modèle Langmuir.

Kurzreferat – Adsorptionsstudien unter Verwendung von N_2 (78°K), H_2O (273°K) und $BuNH_2$ (298°K) wurden an Georgia Kaolinen mit einem weiten Kristallinitäts – und Teilchengrössenbereich (von 0·1μ bis 44μ) durchgeführt. Unter Verwendung von Adsorptionsverfahren in der Dampf – sowie in der Flüssigphase wurden die Oberflächenaffinitäten der Adsorbate bestimmt. Es wurden modifizierte Frenkel–Halsey–Hill Diagramme verwendet um das bevorzugte Adsorptionsvermögen von Wasserdampf gegenüber N_2 (Hydrophilie Index H.I.) als eine Funktion des Kristallinitätsindexes, C.I., und der Teilchengrösse zu errechnen. Für das Adsorptionsvermögen von Amin wurden nichtwässrige Adsorptionsisothermem erhalten. Innerhalb einer geographischen Ablagerung irgendwelcher Art zeigt die Kristallinität einen inkonsequenten Verlauf in Bezug auf die Teilchengrösse. Allgemein ist allein die Neigung der Kristallinität in der Richtung zum Bereich der feinen Teilchen $\bar{D} \rightarrow 0.2\mu$ hin zuzunehmen. Die Adsorptionsvermögen von N_2, H_2O und $BuNH_2$ zeigen innerhalb eines gegebenen Bereiches von Teilchengrössen keine Abhängigkeit von der Kristallinität F.H H.-kompensierte Verläufe, die das bevorzugte Adsorptions-vermögen gegenüber N_2 beschreiben, zeigen jedoch eine deutliche Abnahme bei zunhmender Kristallinität Eine auffallende Anormalität tritt in der Nähe von $0{,}2 < C.I. < 0{,}7$ auf wo H.I. kurz zunimmt und dann wieder der ursprünglichen Tendenz zu folgen. Die Geschwindigkeit der Abnahme von H.I. gegenüber C.I. ist durchwegs steiler mit zunehmender

https://doi.org/10.1346/CCMN.1970.0180105 Published online by Cambridge University Press

Teilchengrösse. Die Adsorption von Wasserdampf erfolgt wahrscheinlich als 1 : 1 Konfiguration an jeder Kieselerde-Tonerde Randgruppe, 1 : 1 an jeder Basiskieselerde und 1 : 2 (verhinderte Konfiguration) an jeder Basistonerdegruppe. Die Messwerte deuten darauf hin, dass Amine vorzugsweise und quantitativ an den Kanten, d.h. den Stellen der Lewis und Bronsted Säuren adsorbieren, und einem Langmuir Muster folgen.

Резюме—Исследования адсорбции выполнены на образцах каолинита из Джорджии, характеризующихся низкими пределами кристалличности и размерами частиц (от 0,1 до 44 мк), с использованием N_2 (78 °K), H_2O (273 °K) и $BuNH_2$ (298 °K). С. помощью методов адсорбции как паров, так и жидкой фазы определены величины поверхностного сродства адсорбатов. С помощью видоизмененных кривых Френкеля-Хелси-Хилла (ФХХ) подсчитаны величины преимущественной адсорбции паров H_2O по сравнению с N_2 (индекс гидрофильности, ИГ) как функции индекса кристалличности (ИК) и размеров частиц. Получены изотермы безводной адсорбции для поглощения аминов.

Для каждого месторождения степень кристалличности не находится в закономерной связи с размером частиц. Наблюдается лишь единственная общая тенденция увеличения степени кристалличности при приближении размеров частиц к величинам $\overline{D} \rightarrow 0,2$ мк. Поглощаемость N_2, H_2O и $BuNH_2$ не обнаруживает никакой зависимости в пределах какого-либо заданного интервала размеров частиц. Однако скомпенсированные наклоны кривых ФХХ, описывающих преимущественную адсорбцию по сравнению с N_2, уменьшаются при увеличении степени кристалличности. Удивительная аномалия наблюдается вблизи интервала $0,2 < ИК < 0,7$, где ИГ на узком участке возрастает, но затем снова вос первоначальнае тенденция. Скорость уменьшения ИГ в зависимости от ИК неизменно больше при увеличении размеров частиц. Поглощение паров воды скорее происходят в виде конфигурацией 1:1 на каждой краевой Si–Al-группе, 1:1 на каждой базальной Si–группе и 1:2 (задняя конфигурация)–на каждой базальной Al— группе.

Данные указывают, что амины поглощаются преимущественно и количественно на краях, т.е. на кислотных положениях Люиса и Бронстеда в соответствии с Ленгмюровской картиной.

https://doi.org/10.1346/CCMN.1970.0180105 Published online by Cambridge University Press